Published in final edited form as:
Optom Vis Sci. 2010 January ; 87(1): 28–36. doi:10.1097/OPX.0b013e3181c61117.

Determinants of Contrast Sensitivity for the Tumbling E and Landolt C

Kenneth R. Alexander, PhD[1,2,3] and **J. Jason McAnany, PhD**[1]

[1] Department of Ophthalmology and Visual Sciences, University of Illinois at Chicago, Chicago, Illinois

[2] Department of Psychology, University of Illinois at Chicago, Chicago, Illinois

[3] Department of Bioengineering, University of Illinois at Chicago, Chicago, Illinois

Abstract

Purpose—To compare the object spatial frequencies that underlie contrast sensitivity for the tumbling E and Landolt C across a range of optotype sizes and under conditions biased toward the magnocellular (MC) and parvocellular (PC) pathways.

Methods—Contrast thresholds of two visually normal observers were measured using tumbling E optotypes that were either low-pass filtered or high-pass filtered with a two-dimensional Gaussian filter. Optotypes were presented using steady-pedestal and pulsed-pedestal paradigms to target the MC and PC pathways, respectively. Object frequencies essential for orientation judgments of the tumbling E were derived from plots of log contrast threshold vs. log filter cutoff frequency, and results were compared to those obtained previously for the Landolt C under identical testing conditions.

Results—The object frequency used to judge the orientation of the tumbling E increased systematically with increasing target angular subtense, and the effect of target size differed depending on whether performance was mediated by the inferred MC or PC pathway. The overall pattern of results was similar for the tumbling E and Landolt C, but there was generally less dependence of object frequency on target angular subtense for the tumbling E.

Conclusions—The tumbling E and Landolt C are not equivalent in terms of the object frequencies that mediate orientation judgments. However, both optotypes show scale-dependent changes in object frequency, particularly under test conditions that favor the PC pathway. The scale dependence of these broadband optotypes can pose a challenge in interpreting test results using these targets. A potential solution is to use spatially filtered optotypes with limited, known object frequency content.

Keywords

Contrast Sensitivity; Spatial Frequency; Visual Acuity; Optotype; Magnocellular; Parvocellular

In the clinical setting, visual performance has traditionally been evaluated using letter optotypes. Letters have the advantage of being familiar to patients, but the individual letters are not necessarily all equally identifiable,[1,2] which can potentially lead to variability in test results. An alternative optotype is the Landolt C, which has been adopted as the standard for visual acuity testing[3,4] and has also been used to evaluate contrast sensitivity.[5–7] However, a

Corresponding author: Kenneth R. Alexander, Department of Ophthalmology and Visual Sciences, University of Illinois at Chicago, 1855 West Taylor Street, Chicago, IL 60612. Fax: (312) 996-7770; kennalex@uic.edu.

potential drawback to the use of the Landolt C is that its curved features can make it difficult to produce on video displays without aliasing and distortion, especially at small optotype sizes.

A potentially useful alternative to the Landolt C is the tumbling E, which can be produced more readily on video displays owing to its linear features. In addition, the repeating bar pattern of the tumbling E renders it intermediate between letters and grating stimuli.[8] As is the case for the Landolt C, orientation judgments of the tumbling E are easily incorporated into a forced-choice paradigm and the optotype is useful for patients unfamiliar with the Latin alphabet. The tumbling E has been used primarily in the clinical assessment of visual acuity[9,10] and it has not been used to measure contrast sensitivity per se, although it has been used to evaluate low-contrast visual acuity in studies of the effect of optical aberrations on visual performance.[11,12] Given its grating-like characteristics and its suitability for video displays, the tumbling E may have an advantage over the Landolt C as a clinically useful optotype for evaluating contrast sensitivity, but this remains to be determined.

An important consideration in using the tumbling E and Landolt C optotypes is that, like letter optotypes in general, their Fourier spectra contain a broad range of object spatial frequencies, designated in cycles per letter (cpl).[13] Moreover, as noted by Bondarko and Danilova,14 there is a substantial difference between the Fourier spectra of the tumbling E and Landolt C. For the Landolt C, the peak difference in the amplitude spectra for orthogonal orientations of the optotype occurs near 1.3 cpl. For the tumbling E, on the other hand, the peak difference occurs at 2.5 cpl, which corresponds to the stroke frequency of the bars of the E. The spectral difference between the tumbling E and Landolt C led Bondarko and Danilova14 to suggest that visual acuity might differ for the two optotypes. However, empirical studies have found little difference in visual acuity for the tumbling E and Landolt C in visually normal observers.[15–17] This indicates the differing Fourier spectra of the two optotypes do not have a major influence on visual acuity measurements. It is presently unclear as to how the differing object frequency components of the two optotypes might affect contrast sensitivity. The primary purpose of this study was to investigate this issue.

Previous studies have indicated that there is not a straightforward relationship between object spatial frequency and contrast sensitivity. Originally, it was presumed that a constant band of object spatial frequencies is employed regardless of the visual angle of the optotype.[18] If this were the case, then retinal spatial frequency in cycles per degree (cpd)[13] would scale with optotype size. However, studies have shown that, for letters in general, the identification of small letters is based on low object frequencies, but the identification of large letters is based on high object frequencies.[19–22] Thus, letter identification is not scale invariant. That is, a given change in letter angular subtense does not necessarily entail a proportional change in the retinal spatial frequency of the components that mediate performance. This was also recently found to be the case for orientation judgments for the Landolt C,23 but it remains to be determined whether it is true for the grating-like tumbling E.

A further complication is that the exact relationship between object spatial frequency and contrast sensitivity appears to depend on whether the magnocellular (MC) or parvocellular (PC) contrast-processing stream mediates performance. It is possible to bias contrast sensitivity toward either the MC or PC pathway by using steady-pedestal and pulsed-pedestal paradigms, respectively.[24] Psychophysical data acquired using these two paradigms have the contrast response properties and temporal integration characteristics associated with the MC and PC pathways described electrophysiologically.[25,26] A recent study showed that, for the Landolt C, the dependence of object frequency on target size is greater for testing conditions that favor the PC pathway,23 but it is not clear whether this is also the case for the tumbling E, given that its amplitude spectrum has a prominent component at 2.5 cpl.[14]

Based on these considerations, the aim of the present study was to determine the specific object frequencies that underlie contrast sensitivity for the tumbling E across a range of optotype sizes and under conditions biased toward the MC and PC pathways. The approach was identical to that used to investigate the spatial frequency determinants of orientation judgments for the Landolt C,[23] which, in turn, was based on that of Anderson and Thibos.[27] Specifically, contrast thresholds were measured for tumbling E optotypes that were either low-pass filtered or high-pass filtered using a set of two-dimensional Gaussian filters with a range of cutoff object frequencies. The underlying assumption is that the removal of object frequencies that are irrelevant to orientation judgments should have no effect on contrast threshold, whereas the removal of essential object frequencies will result in a threshold elevation. Contrast thresholds were measured under the steady-pedestal and pulsed-pedestal paradigms to bias performance toward the MC and PC pathways, respectively.[24] The object frequencies that mediated contrast thresholds for the tumbling E derived from this analysis were compared to those obtained previously for the Landolt C.[23]

METHODS

Observers

The same two experienced psychophysical observers as in the previous study of the Landolt C[23] served as subjects (the authors, ages 28 [S_1] and 63 [S_2] years). Both have normal best-corrected visual acuity and contrast sensitivity. S_1 has normal color vision and S_2 has mild deuteranomaly. The experiments were approved by an institutional review board at the University of Illinois at Chicago and the study adhered to the tenets of the Declaration of Helsinki.

Stimuli and Testing System

The test stimulus was an upper case E constructed according to the principles of the Sloan font.[3] The stroke width was 1/5 of the overall optotype size and the three bars were of equal length. The E was of positive contrast (luminance higher than the surround) and it was spatially filtered with either a high-pass or a low-pass two-dimensional Gaussian filter using eleven cutoff object frequencies that ranged from 0.6 to 10 cpl. Fig. 1 presents examples of low-pass-filtered (Fig. 1A) and high-pass-filtered (Fig. 1B) tumbling Es as well as an unfiltered E (Fig. 1C). Four different sizes of tumbling E were used, equivalent to 0.9, 1.2, 1.5, and 1.8 log MAR (minimum angle of resolution, equal to 1/5 the optotype size in arcmin, where smaller values of log MAR correspond to smaller letters). It was not possible to make meaningful measurements using Es smaller than 0.9 log MAR because contrast thresholds for these smaller optotypes were so elevated under the pulsed-pedestal paradigm that they exceeded the range of available contrasts when the optotypes were filtered.

All stimuli were generated using a Macintosh G4 computer and were displayed on a 22″ NEC monitor (FE2111SB) with a screen resolution of 1280 × 1024 and a 100-Hz refresh rate, driven by an ATI Radeon video card (9000 Pro) with 10-bit DAC resolution. The monitor, which was the only source of illumination in the room, was viewed monocularly from 1.9 meters through a phoropter with the observer's best refractive correction. Experiments were written in Matlab using the Psychophysics Toolbox extensions.[28]

Steady-pedestal and pulsed-pedestal paradigms,[24] illustrated in Fig. 2, were used to bias performance toward the MC and PC pathways. For both paradigms, the test stimulus was presented in the center of a luminance pedestal that subtended 10.4° horizontally and 8.5° vertically. The luminance pedestal was presented in the center of an adapting field that subtended 11.0° horizontally and 8.8° vertically. Four diagonal black lines that extended from the edges of the pedestal to a region just outside of the tumbling E were presented continuously

to aid fixation. The pedestal luminance was 30 cd/m^2, and it was added to an adapting field of 30 cd/m^2, so that the luminance of the pedestal plus adapting field was 60 cd/m^2.

For the steady-pedestal paradigm (Fig. 2, top), the luminance pedestal was presented continuously in the center of the adapting field. During the test period, the target was presented briefly in the center of the pedestal. This paradigm is thought to favor the MC pathway, at least for large target sizes, because the test target is presented only briefly. For the pulsed-pedestal paradigm (Fig. 2, bottom), the pedestal and test target were presented briefly and simultaneously. This paradigm is thought to favor the PC pathway, because the abrupt onset of the luminance pedestal drives the MC pathway toward saturation.

The test stimulus duration was 30 ms (3 video frames), which was chosen to be within the temporal integration time of the inferred MC and PC pathways.[29] The temporal characteristics of the display were confirmed using an oscilloscope and photocell. The luminance values used to generate the stimuli were determined by a linearized look-up table, based on calibrations made with a Minolta LS-110 photometer. The contrast (C) of the unfiltered tumbling E was defined as Weber contrast:

$$C=(L_T - L_P)/L_P, \quad (1)$$

where L_T is the luminance of the tumbling E and L_P is the luminance of the pedestal plus adapting field. Because the contrast of complex images is difficult to define,[30] a relative definition of contrast was used to characterize the filtered tumbling E, as in previous studies.[20,21,23] That is, when the contrast of the original unfiltered tumbling E was 1.0, the filtered image was assigned a relative contrast of 1.0 without rescaling.

Procedure

A 30-s period of adaptation to the adapting field alone (pulsed-pedestal paradigm) or to the adapting field plus pedestal (steady-pedestal paradigm) preceded each session, and a brief warning tone signaled the start of each stimulus presentation. On each trial, the bars of the tumbling E faced randomly either toward the right or upward, yielding a two-alternative forced-choice procedure. These two alternatives were used rather than a four-alternative procedure because right-left and up-down judgments of the tumbling E involve a phase discrimination (although this is likely to be an important factor only in non-foveal measurements8). The observer's task was to determine the orientation of the tumbling E. No feedback was given. Contrast thresholds for orientation judgments were obtained using the QUEST procedure,31 with the number of trials set to 40 for each condition.

Within a given testing session, all cutoff object frequencies for both the high-pass-filtered and low-pass-filtered targets were presented at a fixed target size under either the steady-pedestal or the pulsed-pedestal paradigm. The paradigms, sizes, and cutoff object frequencies were presented in a pseudo-random order, and each condition was tested three times in separate sessions. The three estimates of threshold for each condition were then averaged for each observer. Because the results for the two observers were highly similar (as in the previous study of the Landolt C23), the data were averaged, and the plotted points in the figures represent the means for the two observers.

RESULTS

Effect of Gaussian Filtering on Contrast Thresholds

Fig. 3 illustrates the effect of low-pass and high-pass Gaussian filtering on log contrast thresholds for the tumbling E (Figs. 3A, 3B) and Landolt C (Figs. 3C, 3D), each with a log

MAR value of 1.5, which corresponds to the letter size used in the Pelli-Robson contrast sensitivity chart. Data were acquired using either the steady-pedestal paradigm (Figs. 3A, 3C) or the pulsed-pedestal paradigm (Figs. 3B, 3D). The leftmost data point for the high-pass conditions (filled symbols) and the rightmost data point for the low-pass conditions (open symbols) represent the threshold values for targets that were minimally filtered. The other data points represent the effect of successively changing the cutoff object frequency of the filter to remove either the low object frequencies (high-pass filtering) or the high object frequencies (low-pass filtering). It is apparent from Fig. 3 that, as the filter cutoff frequency was varied, there was no effect on contrast threshold until a critical object frequency was reached. Then, the further removal of object frequencies resulted in a systematic elevation of the log contrast threshold.

In order to derive a quantitative estimate of the object frequency range important for orientation judgments, the data in each plot of Fig. 3 were fit piecewise with two linear functions using a least-squares criterion: one region was constrained to have a slope of 0, and the slope of the second region was unconstrained. The high-pass and low-pass functions in each plot were fit separately. The cutoff object frequency at which the functions crossed (indicated by the vertical dashed lines) was taken as the index of the center of the object frequency region required for orientation judgments. This point represents equal elevations of the log contrast threshold compared to the threshold values obtained with minimally filtered optotypes. The data of Fig. 3 indicate that the range of useful object frequencies (difference between the knee-points of the functions) was approximately 0.5 log units (1.67 octaves) for both optotypes and both paradigms. This value agrees well with the value of 1.6 ±0.7 reported previously for a number of different test targets but obtained with a different technique.[22]

For both optotypes, log contrast thresholds were higher overall for the pulsed-pedestal paradigm than for the steady-pedestal paradigm, as is typical for these two paradigms.[24] Furthermore, the non-horizontal lines that were fit to the data for the steady-pedestal paradigm (Figs. 3A, 3C) had a steeper slope than those fit to the data for the pulsed-pedestal paradigm (Figs. 3B, 3D). It is likely that this slope difference is related to the slopes of the CSFs of the inferred MC and PC pathways, which differ over the spatial frequency range examined here. For example, the relatively steeper slope of the CSF for the inferred MC pathway at intermediate spatial frequencies[24] means that a small change in spatial frequency due to filtering would entail a relatively large change in contrast threshold. This would account for the steeper slopes of the non-horizontal portions of the functions fit to the data of the steady-pedestal paradigm.

Log contrast thresholds were slightly higher overall for the Landolt C than for the tumbling E. Nevertheless, for the steady-pedestal paradigm, the center object frequency was similar for both optotypes (approximately 2.4 cpl for the tumbling E vs. 2.2 cpl for the Landolt C). For the pulsed-pedestal paradigm, however, the center object frequency differed for the two optotypes (approximately 3.0 cpl for the tumbling E vs. 3.9 cpl for the Landolt C). The fact that center object frequencies were higher for the pulsed-pedestal than for the steady-pedestal paradigm indicates that edge information is more important for orientation judgments made under the pulsed-pedestal paradigm.

Center Object Frequency as a Function of Optotype Size

The analysis illustrated in Fig. 3 was then applied to the data obtained at each of the optotype sizes, except that the data of each observer were fit separately to obtain an estimate of the center object frequency for that observer at that size. The results for the two observers were then averaged, and the mean results are shown in Fig. 4. This figure plots the mean log center object frequency for the two observers as a function of the log of the reciprocal of MAR for the tumbling E (Fig. 4A) and Landolt C (Fig. 4B) for both the steady-pedestal (circles) and pulsed-

pedestal (triangles) paradigms. The reciprocal of MAR was used so that the results for small letters would be plotted to the right along the *x*-axis, which is the conventional orientation of a CSF. The horizontal dashed line in Fig. 4 is a reference line that is based on the assumption that orientation judgments are based on a constant object frequency of 2.5 cpl (corresponding to the stroke width), regardless of target size.

Each data set was separately fit with the log form of the equation:

$$F_o = F_{o_{\min}}(1+(MAR_{crit}/MAR)), \tag{2}$$

where F_o indicates the center object frequency, $F_{o_{min}}$ represents the asymptotic object frequency at small optotype sizes, and MAR_{crit} is the value of MAR at which F_o is twice $F_{o_{min}}$. On log-log coordinates, the function described by Eq. 2 transitions between a slope of −1 for large optotypes (which represents a constant retinal frequency) to a slope of 0 for small optotypes (which represents a constant object frequency), and $F_{o_{min}}$ and MAR_{crit} control the vertical and horizontal positions of the function, respectively. The parameters derived from the fits of Eq. 2 to the data are given in linear units in Table 1.

There was an overall similarity between the functions for the tumbling E (Fig. 4A) and the Landolt C (Fig. 4B). For large optotype sizes (leftmost data points in each plot), the center object frequency was markedly higher under the pulsed-pedestal paradigm (triangles) than under the steady-pedestal paradigm (circles). As the optotype size decreased, the center object frequencies became more similar under the two paradigms for both optotypes. However, the functions were flatter overall for the tumbling E than for the Landolt C, as reflected in the larger values of MAR_{crit} for the tumbling E (Table 1). Furthermore, the difference between the functions for the steady-pedestal and pulsed-pedestal paradigms was smaller for the tumbling E than for the Landolt C. In addition, the values of $F_{o_{min}}$ for both paradigms were slightly larger for the tumbling E than for the Landolt C (Table 1). This indicates that orientation judgments at the acuity limit would be based on a slightly higher object frequency for the tumbling E.

The relationship between center object frequency and retinal spatial frequency for the two optotypes is shown in Fig. 5. This figure replots the data and best-fit curves of Fig. 4 in terms of retinal frequency F_r in cpd, based on the relationship:

$$F_r = \frac{12^* F_o}{MAR}. \tag{3}$$

Fig. 5 also provides a more direct comparison of the results for the tumbling E and Landolt C.

The top *x*-axes in Fig. 5 indicate the nominal retinal frequencies corresponding to the log MAR values. This correspondence is based on the convention that 0 log MAR (20/20 Snellen equivalent) is equivalent to a retinal frequency of 30 cpd.[18] This relationship is based in turn on the assumption that F_o equals 2.5 cpl, equivalent to the stroke width. The diagonal dashed line in Fig. 5 represents a one-to-one relationship between the nominal retinal frequency and the derived center retinal frequency. If orientation judgments for the tumbling E and Landolt C are, in fact, governed by an object frequency range centered on 2.5 cpl for all optotype sizes, then the nominal retinal frequency would be proportional to log MAR and the data would fall along the dashed line.

Under the steady-pedestal paradigm (Fig. 5A), which targets the MC pathway, the results were similar for both the tumbling E and the Landolt C. However, the data for the tumbling E tended

to be closer overall to the dashed line than were the results for the Landolt C. For the smaller targets, the functions approached a slope of 1 for both optotypes, indicating that log retinal frequency was nearly proportional to log MAR. Thus, a nearly constant object frequency was employed for orientation judgments for both targets at the smaller optotype sizes under the steady-pedestal paradigm. However, the data points for the smaller log MAR values fell below the dashed line, which indicates that the observers used object frequencies below 2.5 cpl for orientation judgments for both the Landolt C and tumbling E at the smaller optotype sizes.

For the pulsed-pedestal paradigm (Fig. 5B), which emphasizes the PC pathway, there was a greater divergence of the derived retinal frequencies from the nominal retinal frequencies than was the case for the steady-pedestal paradigm. For the largest optotypes, the derived retinal frequency was considerably higher than the nominal retinal frequency, although the difference was less for the tumbling E than for the Landolt C. For the smaller optotypes, however, the derived retinal frequency was *lower* than the nominal retinal frequency for both optotypes, as was also the case for the steady-pedestal paradigm.

DISCUSSION

The purpose of this study was to define the object frequencies that underlie contrast sensitivity for the tumbling E in comparison to previous results for the Landolt C.[23] We observed that, for the tumbling E, as for the Landolt C, the object frequency band that governed contrast sensitivity varied systematically with the log MAR value of the optotype (Fig. 4). As a result, retinal frequency did not vary in strict proportion to the angular subtense of the targets (Fig. 5). Therefore, even though the tumbling E has grating-like characteristics, it still shows scale dependence of object frequencies. This is perhaps not surprising, given previous evidence that a square-wave grating itself shows scale dependence.[22]

Our results show further that, for both the tumbling E and Landolt C, the magnitude of the scale dependence varied with the nature of the contrast-processing pathway that mediated contrast sensitivity. For both optotypes, contrast sensitivity was based on higher object frequencies for the pulsed-pedestal paradigm (inferred PC pathway) than for the steady-pedestal paradigm (inferred MC pathway), particularly at large optotype sizes. The change in object frequency with target size was generally slightly less for the tumbling E than for the Landolt C (Fig. 4A vs Fig. 4B). The greatest difference between the two optotypes occurred for the largest targets presented under the pulsed-pedestal paradigm, where the object frequency was 0.15 log units (factor of 1.4) higher for the Landolt C than for the tumbling E.

As discussed previously,23 the fact that object frequencies were different for the steady-pedestal and pulsed-pedestal paradigms at large optotype sizes is likely due to the differing shapes of the CSFs of the inferred MC and PC pathways.[24] The inferred MC pathway, which has a low-pass CSF, has a relatively high sensitivity for the low object frequency components of large optotypes, which correspond to low retinal frequencies. Thus, for large, briefly presented optotypes, contrast sensitivity can be based on relatively low object frequencies if sensitivity is mediated by the inferred MC pathway. However, the inferred PC pathway, which has a band-pass CSF, has a reduced sensitivity for these low-frequency components. Therefore, orientation judgments using large optotypes would necessarily be based on higher object frequencies under the pulsed-pedestal paradigm (inferred PC pathway) than under the steady-pedestal paradigm (inferred MC pathway), as is observed in Fig. 4.

For optotype sizes that are near the acuity limit, on the other hand, the high object frequency components of the targets, which correspond to high retinal frequencies, would exceed the contrast sensitivity limits for both pathways. Consequently, orientation judgments would necessarily be based on relatively low object frequencies for both paradigms when the targets

are small. However, object frequencies below approximately 1 cpl contain little information about target orientation,[14] as is apparent from Fig. 1. Therefore, there is a restricted range of useful object frequencies for targets of small angular subtense, and this limited range is similar for both the inferred MC and inferred PC pathway. This would account for the fact that the functions for the steady- and pulsed-pedestal paradigms shown in Fig. 4 tended to converge at small optotype sizes for both the tumbling E and Landolt C.

The values of $F_{o_{min}}$ (asymptotic object frequency at small optotype sizes) shown in Table 1 were only slightly higher for the tumbling E than for the Landolt C. This difference equates to a slightly worse visual acuity (larger value of log MAR by approximately 0.1 log unit) for the tumbling E. Previous studies have similarly found little if any difference in visual acuity for the tumbling E vs. Landolt C[15–17] despite the marked differences in the amplitude spectra of these optotypes.14 Of note, the values of $F_{o_{min}}$ were substantially less than the 2.5 cpl that might be expected based on the stroke width of the optotypes. This finding is in agreement with previous studies that specifically investigated the object frequencies that govern visual acuity for the tumbling E[27] and Landolt C.[32] The fact that orientation judgments for both the tumbling E and Landolt C are based on object frequencies lower than 2.5 cpl for target sizes near the acuity limit indicates that observers do not use the stroke width or gap width to judge the orientation of these optotypes. Instead, orientation judgments of the tumbling E and Landolt C at the acuity limit are based on the shape of the light distribution in an effectively low-pass filtered image.

Our results have important implications for clinical tests of contrast sensitivity. The first issue is that of viewing duration. The present study employed brief presentation durations in order to distinguish between the contrast sensitivities of the inferred MC and PC pathways. However, clinical contrast sensitivity tests, such as the Pelli-Robson chart, typically employ unlimited viewing, and observers are often encouraged to stare at the optotypes. At long stimulus durations, however, the sensitivities of the inferred MC and PC pathways are approximately equal.[29] Therefore, there is some uncertainty as to the visual pathway that mediates performance at long durations. The low stimulus contrast may favor the MC pathway, but the long viewing duration may favor the PC pathway. It would seem advisable to limit the exposure duration of the targets, so that there is less ambiguity as to which contrast processing pathway is mediating performance.

A second issue concerns the lack of a fixed relationship between retinal frequency and the angular size of the tumbling E and Landolt C optotypes (Fig. 5). This is a particular problem under conditions targeting the PC pathway (pulsed-pedestal paradigm), where the retinal frequency used for orientation discrimination tends to be relatively constant even though the target size is varied (Fig. 5B). This is a lesser issue under conditions favoring the MC pathway (steady-pedestal paradigm), where there is a smaller disparity between the nominal and actual retinal frequencies (Fig. 5A). This scale dependence can pose a potential problem in the interpretation of clinical contrast sensitivity measurements using these optotypes. This may be a particular consideration in patients with retinal diseases, who may have spatial-frequency-dependent changes in contrast sensitivity.[e.g.,33,34] Retinal pathology may require such patients to use different object frequencies with potentially different information content compared to visually normal observers.

As discussed previously,[23] a potential solution to the problem of scale dependence is to employ optotypes that are restricted in their spatial frequency content, either through band-pass filtering that limits the object frequency content to a specific spectral region, or through high-pass filtering that effectively prevents observers from using low object frequencies. If such spatially filtered optotypes are employed, then observers do not have the option of using arbitrary object frequencies as the basis for orientation judgments. In fact, optotypes that are effectively high-

pass filtered have been proposed as an improved method for measuring visual acuity.[35–37] However, the optimum region of object frequencies to be used in clinical tests of contrast sensitivity remains to be determined.

Acknowledgments

Disclosure of Funding: NIH research grant EY008301 (KRA), NIH Core Grant EY001792, and a Senior Scientific Investigator Award (KRA) and unrestricted departmental grant from Research to Prevent Blindness, Inc.

References

1. Alexander KR, Xie W, Derlacki DJ. Visual acuity and contrast sensitivity for individual Sloan letters. Vision Res 1997;37:813–819. [PubMed: 9156226]
2. Raasch TW, Bailey IL, Bullimore MA. Repeatability of visual acuity measurement. Optom Vis Sci 1998;75:342–348. [PubMed: 9624699]
3. National Research Council Committee on Vision. Recommended standard procedures for the clinical measurement and specification of visual acuity. Adv Ophthalmol 1980;41:103–148. [PubMed: 7001873]
4. International Organization for Standardization. Visual Acuity Testing: Method of Correlating Optotypes, ISO 8597:1994. Geneva, Switzerland: International Organization for Standardization; 1994. Optics and Optical Instruments.
5. Dennis RJ, Beer JM, Baldwin JB, Ivan DJ, Lorusso FJ, Thompson WT. Using the Freiburg Acuity and Contrast Test to measure visual performance in USAF personnel after PRK. Optom Vision Sci 2004;81:516–524.
6. Bühren J, Terzi E, Bach M, Wesemann W, Kohnen T. Measuring contrast sensitivity under different lighting conditions: Comparison of three tests. Optom Vision Sci 2006;83:290–298.
7. Bach M. The Freiburg Visual Acuity Test – Variability unchanged by post-hoc re-analysis. Graefes Arch Clin Exp Ophthalmol 2007;245:965–971. [PubMed: 17219125]
8. Anderson RS, Thibos LN. Relationship between acuity for gratings and for tumbling-E letters in peripheral vision. J Opt Soc Am A 1999;16:2321–2333.
9. González EG, Tarita-Nistor L, Markowitz SN, Steinbach MJ. Computer-based test to measure optimal visual acuity in age-related macular degeneration. Invest Ophthalmol Vis Sci 2007;48:4838–4845. [PubMed: 17898311]
10. Bourne RR, Rosser DA, Sukudom P, et al. Evaluating a new logMAR chart designed to improve visual acuity assessment in population-based surveys. Eye 2003;17:754–758. [PubMed: 12928690]
11. Yoon G, Jeong TM, Cox IG, Williams DR. Vision improvement by correcting higher-order aberrations with phase plates in normal eyes. J Refract Surg 2004;20:S523–S527. [PubMed: 15523969]
12. Villegas EA, Alcón E, Artal P. Optical quality of the eye in subjects with normal and excellent visual acuity. Invest Ophthalmol Vis Sci 2008;49:4688–4696. [PubMed: 18552387]
13. Parish DH, Sperling G. Object spatial frequencies, retinal spatial frequencies, noise, and the efficiency of letter discrimination. Vision Res 1991;31:1399–1415. [PubMed: 1891827]
14. Bondarko VM, Danilova MV. What spatial frequency do we use to detect the orientation of a Landolt C? Vision Res 1997;37:2153–2156. [PubMed: 9327062]
15. Bennett AG. Ophthalmic test types. A review of previous work and discussions on some controversial questions. Br J Physiol Opt 1965;22:238–271. [PubMed: 5331332]
16. Grimm W, Rassow B, Wesemann W, Sauer K, Hilz R. Correlation of optotypes with the Landolt ring – a fresh look at the comparability of optotypes. Optom Vis Sci 1994;71:6–13. [PubMed: 8146001]
17. Reich LN, Ekabutr M. The effects of optical defocus on the legibility of the Tumbling-E and Landolt-C. Optom Vision Sci 2002;79:389–393.
18. Regan D, Raymond J, Ginsburg AP, Murray TJ. Contrast sensitivity, visual acuity and the discrimination of Snellen letters in multiple sclerosis. Brain 1981;104:333–350. [PubMed: 7237098]
19. Thorn F, Schwartz F. Effects of dioptric blur on Snellen and grating acuity. Optom Vis Sci 1990;67:3–7. [PubMed: 2308749]

20. Alexander KR, Xie W, Derlacki DJ. Spatial-frequency characteristics of letter identification. J Opt Soc Am A 1994;11:2375–2382.
21. Chung ST, Legge GE, Tjan BS. Spatial-frequency characteristics of letter identification in central and peripheral vision. Vision Res 2002;42:2137–2152. [PubMed: 12207975]
22. Majaj NJ, Pelli DG, Kurshan P, Palomares M. The role of spatial-frequency channels in letter identification. Vision Res 2002;42:1165–1184. [PubMed: 11997055]
23. McAnany JJ, Alexander KR. Spatial frequencies used in Landolt C orientation judgments: relation to inferred magnocellular and parvocellular pathways. Vision Res 2008;48:2615–2624. [PubMed: 18374385]
24. Leonova A, Pokorny J, Smith VC. Spatial frequency processing in inferred PC- and MC-pathways. Vision Res 2003;43:2133–2139. [PubMed: 12855249]
25. Kaplan E, Shapley RM. The primate retina contains two types of ganglion cells, with high and low contrast sensitivity. Proc Natl Acad Sci USA 1986;83:2755–2757. [PubMed: 3458235]
26. Lee BB. Receptive field structure in the primate retina. Vision Res 1996;36:631–644. [PubMed: 8762295]
27. Anderson RS, Thibos LN. Sampling limits and critical bandwidth for letter discrimination in peripheral vision. J Opt Soc Am A 1999;16:2334–2342.
28. Brainard DH. The psychophysics toolbox. Spat Vision 1997;10:433–436.
29. Pokorny J, Smith VC. Psychophysical signatures associated with magnocellular and parvocellular pathway contrast gain. J Opt Soc Am A 1997;14:2477–2486.
30. Peli E. Contrast in complex images. J Opt Soc Am A 1990;7:2032–2040. [PubMed: 2231113]
31. Watson AB, Pelli DG. QUEST: a Bayesian adaptive psychometric method. Percept Psychophys 1983;33:113–120. [PubMed: 6844102]
32. Hess RF, Dakin SC, Kapoor N. The foveal ‘crowding’ effect: physics or physiology? Vision Res 2000;40:365–370. [PubMed: 10820616]
33. Alexander KR, Barnes CS, Fishman GA, Pokorny J, Smith VC. Contrast processing deficits in melanoma-associated retinopathy (MAR). Invest Ophthalmol Vis Sci 2004;45:305–310. [PubMed: 14691188]
34. Alexander KR, Barnes CS, Fishman GA. Characteristics of contrast processing deficits in X-linked retinoschisis. Vision Res 2005;45:2095–2107. [PubMed: 15845241]
35. Howland B, Ginsburg A, Campbell F. High-pass spatial frequency letters as clinical optotypes. Vision Res 1978;18:1063–1066. [PubMed: 706157]
36. Frisén L. Vanishing optotypes. New type of acuity test letters. Arch Ophthalmol 1986;104:1194–1198. [PubMed: 3741251]
37. Anderson RS, Ennis FA. Foveal and peripheral thresholds for detection and resolution of vanishing optotype tumbling E’s. Vision Res 1999;39:4141–4144. [PubMed: 10755151]

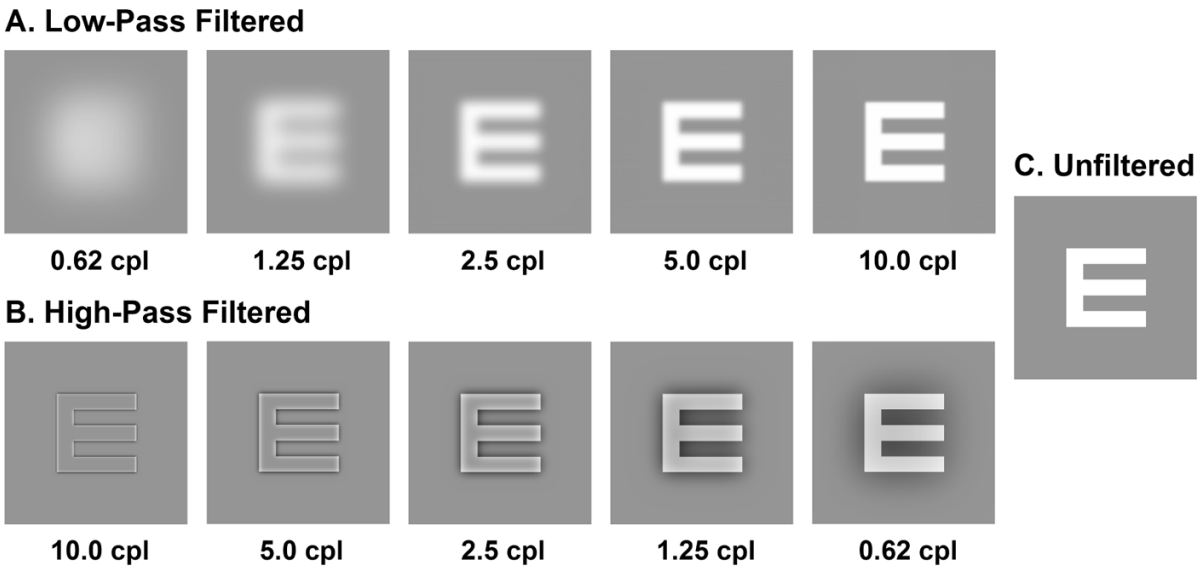

Fig. 1.

Illustrations of a tumbling E that was either low-pass filtered (A) or high-pass filtered (B) with Gaussian filters using the cutoff object frequencies indicated below each image. Images are arranged from most filtered (Ieft) to least filtered (right). An unfiltered optotype (C) is shown for comparison.

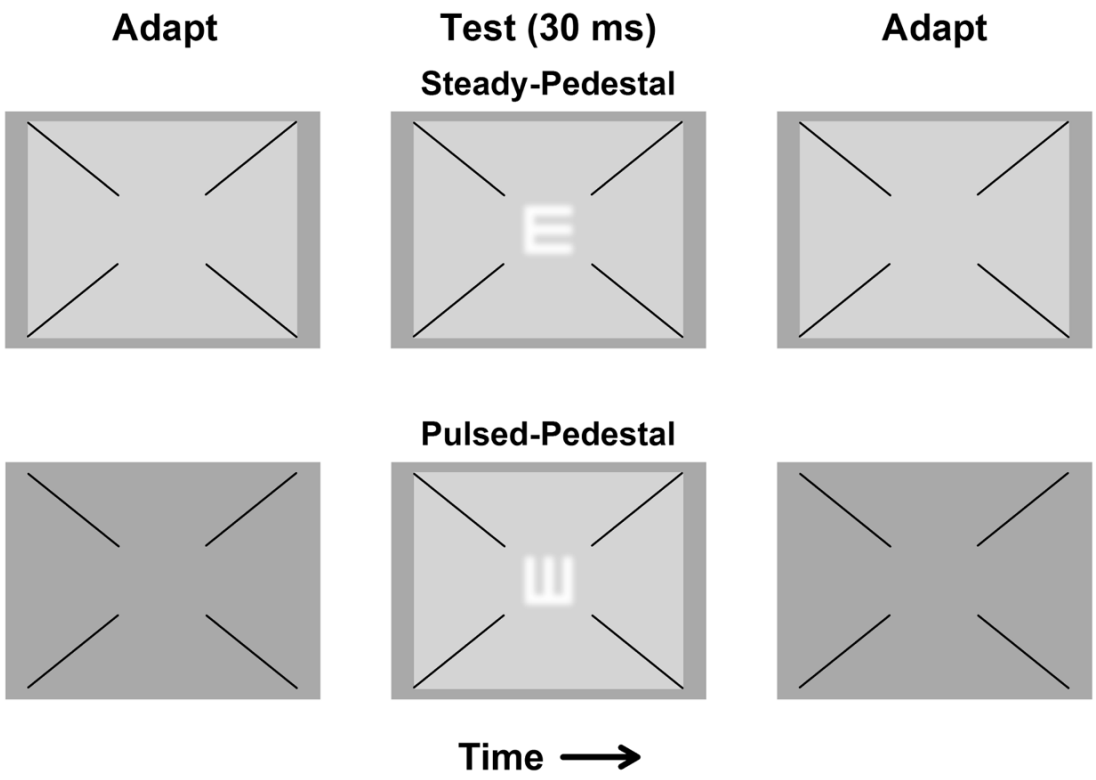

Fig. 2.

Illustration of the steady-pedestal (top) and pulsed-pedestal (bottom) paradigms, shown approximately to scale. For the steady-pedestal paradigm, a pedestal square of incremental luminance was presented continuously against an adapting field. The target was presented briefly during the test interval. For the pulsed-pedestal paradigm, the adapting field was presented continuously, and target and pedestal square were presented briefly and simultaneously during the test interval. For both paradigms, four fixation guides (diagonal lines) that terminated just outside the region of the test target were shown continuously.

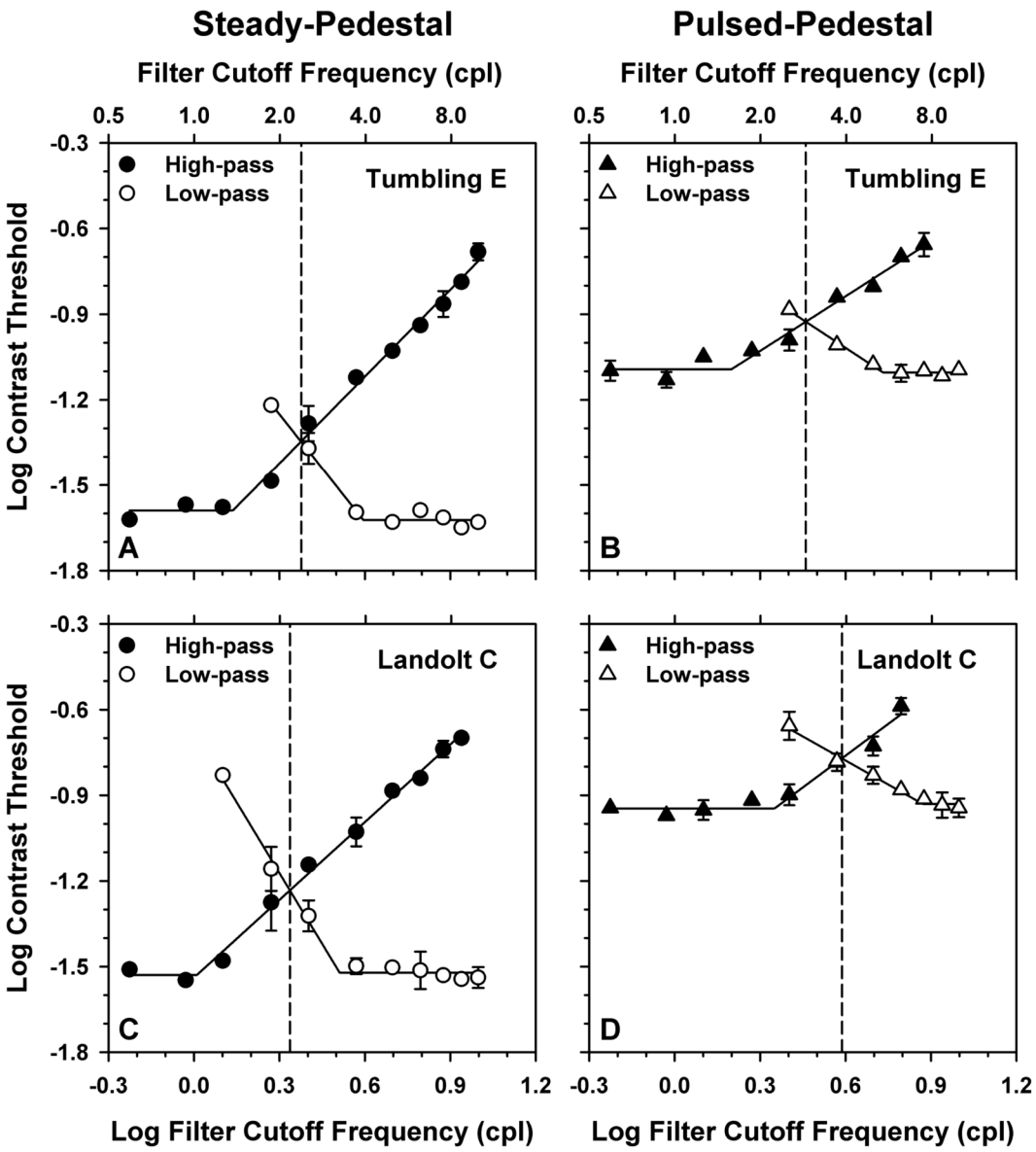

Fig. 3.

Log contrast thresholds for orientation judgments for the tumbling E (A, B) and Landolt C (C, D) as a function of the log object frequency cutoff of a low-pass (open symbols) or high-pass (filled symbols) Gaussian filter, using the steady-pedestal paradigm (A, C) or pulsed-pedestal paradigm (B, D). In this and the following figures, data points represent the means of the two observers and error bars represent ±1 standard error of the mean (sem), which are omitted when smaller than the data points. The solid lines represent piecewise linear fits to the data as described in the text. The dashed vertical lines indicate the point at which the two functions crossed, which was used as the index of the center object frequency.

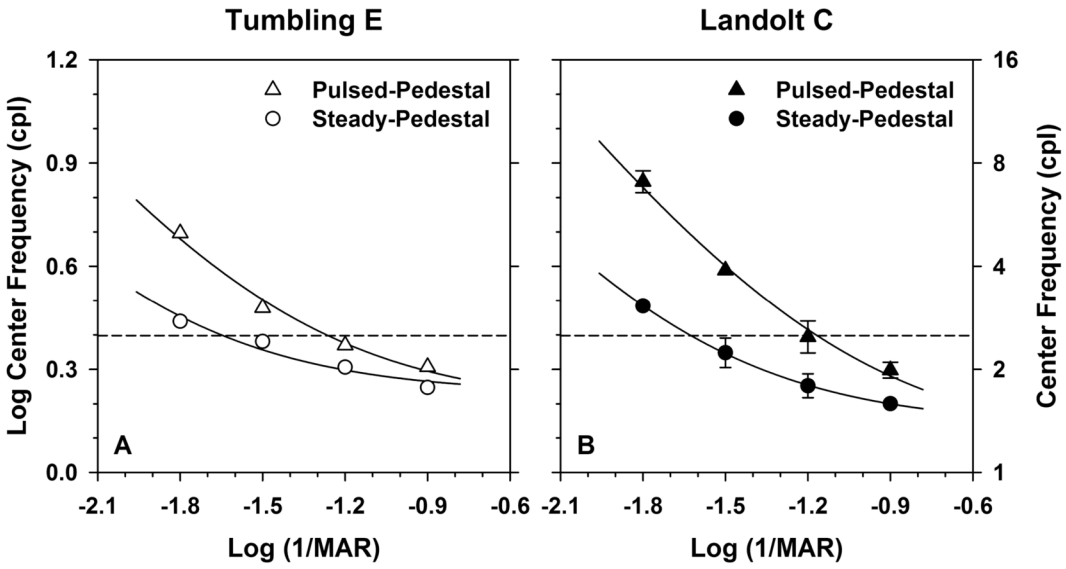

Fig. 4.

Log center object frequency as a function of log reciprocal of MAR for four sizes of tumbling E (A) or Landolt C (B) with data obtained under either the steady-pedestal (circles) or pulsed-pedestal (triangles) paradigm. The right *y*-axis indicates the center object frequency in linear units on a log scale. Curves represent the least-squares best fits of Eq. 2. The dashed horizontal line represents an object frequency of 2.5 cpl.

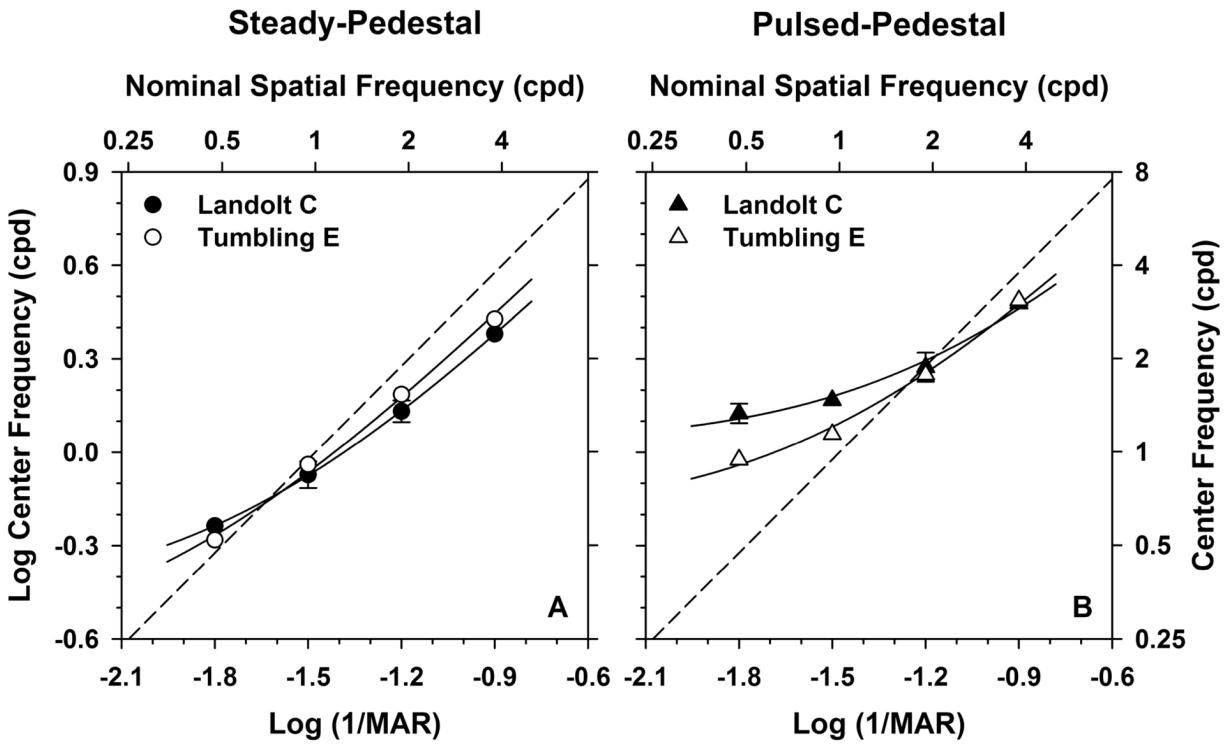

Fig. 5.

Log center object frequency as a function of log reciprocal of MAR for four sizes of tumbling E (A) or Landolt C (B) with data obtained under either the steady-pedestal (circles) or pulsed-pedestal (triangles) paradigm. The data points, curves, and dashed line have been replotted from Fig. 4 in units of cpd rather than cpl, based on Eq. 3. The top *x*-axis indicates the nominal retinal frequency based on the assumption that 0 log MAR equals 30 cpd; the right *y*-axis indicates the center retinal frequency in linear units on a log scale. The diagonal dashed line indicates equality between the nominal and derived retinal frequencies.

TABLE 1

Summary of Parameters Derived from the Best Fits of Eq. 2 to the data of Fig. 4

	$F_{o_{min}}$ (cpl)		MAR_{crit}	
	Steady-Pedestal	**Pulsed-Pedestal**	**Steady-Pedestal**	**Pulsed-Pedestal**
Tumbling E	1.70	1.57	91.20	30.20
Landolt C	1.37	1.21	52.48	13.80